

Self-assembly behavior between native hyaluronan and styrylpyridinium in aqueous solution

Jing Xu^a, Huiyu Bai^{a,*}, Chenglin Yi^a, Jing Luo^a, Cheng Yang^a, Wenshui Xia^b, Xiaoya Liu^{a,b,**}

^a School of Chemical and Material Engineering, Jiangnan University, Wuxi 214122, PR China

^b State Key Laboratory of Food Science and Technology, Jiangnan University, Wuxi 214122, PR China

ARTICLE INFO

Article history:

Received 17 January 2011

Received in revised form 4 May 2011

Accepted 11 May 2011

Available online 18 May 2011

Keywords:

Hyaluronan

Styrylpyridinium

SbQ

Polymer–surfactant interaction

Self-assembly

ABSTRACT

This article reports on the self-assembly behavior of a negatively charged hyaluronan (HA) and an oppositely charged styrylpyridinium species (specifically SbQ) in aqueous solution. Turbidity and Zeta potential measurements were utilized to explore the formation of complex micelles. These nano-sized micellar aggregates have a core–shell structure composed of a hydrophobic inner core containing aggregated SbQ molecules and a hydrophilic HA shell layer. UV spectra and DLS experiments confirmed that the micelles are photo-crosslinkable. A dimerization reaction of the SbQ molecules induced by UV light irradiation led to the crosslinking of the inner core, resulting in a decrease in the size of the micelles.

© 2011 Elsevier Ltd. All rights reserved.

1. Introduction

Hyaluronan (also named hyaluronate, hyaluronic acid or HA) is a naturally occurring polysaccharide originally extracted from bovine vitreous humour, rooster combs or umbilical cords (Rinaudo, 2008), and now has been successfully produced on a large scale by streptococcus bacteria in high purity and good yield (Gao, Du, & Chen, 2006; Ogradowski, Hokka, & Santana, 2005). It consists of repeating β -(1 \rightarrow 4)-D-glucuronic acid β -(1 \rightarrow 3)-N-acetyl-D-glucosamine disaccharide units (Chytil & Pekar, 2009; Cowman & Matsuoka, 2005) (Fig. 1a). Since it is a biopolymer, much current interest focuses on its applications in biomedicine and pharmaceuticals (Lee, Lee, & Park, 2008; Lee, Ahn, & Park, 2009; Pitarresi, Pierro, Palumbo, Tripodo, & Giammona, 2006; Vázquez et al., 2009).

In this work, we focus, in part, on the anionic polyelectrolyte character of HA, allowing it to form electrostatic complexes with cationic compounds. Not surprisingly, many studies are dedicated to HA complexation with oppositely charged compounds, since such complexes provide a path to tailor the properties of HA such as encapsulation capacity, adsorption capacity onto substrate surface

and stability (Kujawa, Moraille, Sanchez, Badia, & Winnik, 2005; Szarpak et al., 2010; Thalberg & Lindman, 1989).

Polyelectrolyte–surfactant systems have been studied intensively for decades due to their potentially useful physicochemical characteristics, and a range of studies are devoted specifically to the interactions between polyelectrolytes and oppositely charged surfactants (Antonietti, 1994; Hansson & Almgren, 1994; Hu, Jonas, Varshney, & Gohy, 2005; Kuntz & Walker, 2007; Leonard & Strey, 2010; Mezei, Mészáros, Varga, & Gilányi, 2007). Several techniques are available to study the interactions between polyelectrolytes and surfactants, such as dynamic and static light scattering (Ren, Gao, Lu, Liu, & Tong, 2006), turbidity (Karlberg, Piculell, & Huang, 2007), small-angle neutron scattering (Annaka, Morishita, & Okabe, 2007; Claesson et al., 2000), surface tension (Kolarié, Jaeger, Hedicke, & Klitzing, 2003), viscometry (Yang, Chen, & Fang, 2009), etc. It is usually accepted that the main driving force for association in polyelectrolyte–surfactant aqueous solution is the hydrophobic interaction as well as electrostatic attraction (Onesippe & Lagerge, 2008; Ren et al., 2006).

SbQ, similar to usual surfactants, is an amphiphilic sensitizer of the styrylpyridinium family. Moreover, it can be dimerized via the [2 + 2]-cycloaddition reaction under UV irradiation (Cockburn, Stephen-Davidson, & Pratt, 1996) (Fig. 1b). According to previous reports, SbQ has been covalently grafted to the polymer poly(vinyl alcohol) (PVA) as a pendant group, and the resulting photo-crosslinkable polymer PVA-SbQ has found widespread use in films, photoresists, biosensors, etc. (Chang, Chang, Chou, Han, & Chen, 2007; Liu, Bolger, Cahill, & McGuinness, 2009; Nam

* Corresponding author. Tel.: +86 510 85917763.

** Corresponding author at: School of Chemical and Material Engineering, Jiangnan University, Wuxi 214122, PR China. Tel.: +86 510 85917763.

E-mail addresses: xujing050201@163.com (J. Xu), bhy.chem@163.com (H. Bai), lxy@jiangnan.edu.cn, lxyjiangnan@126.com (X. Liu).

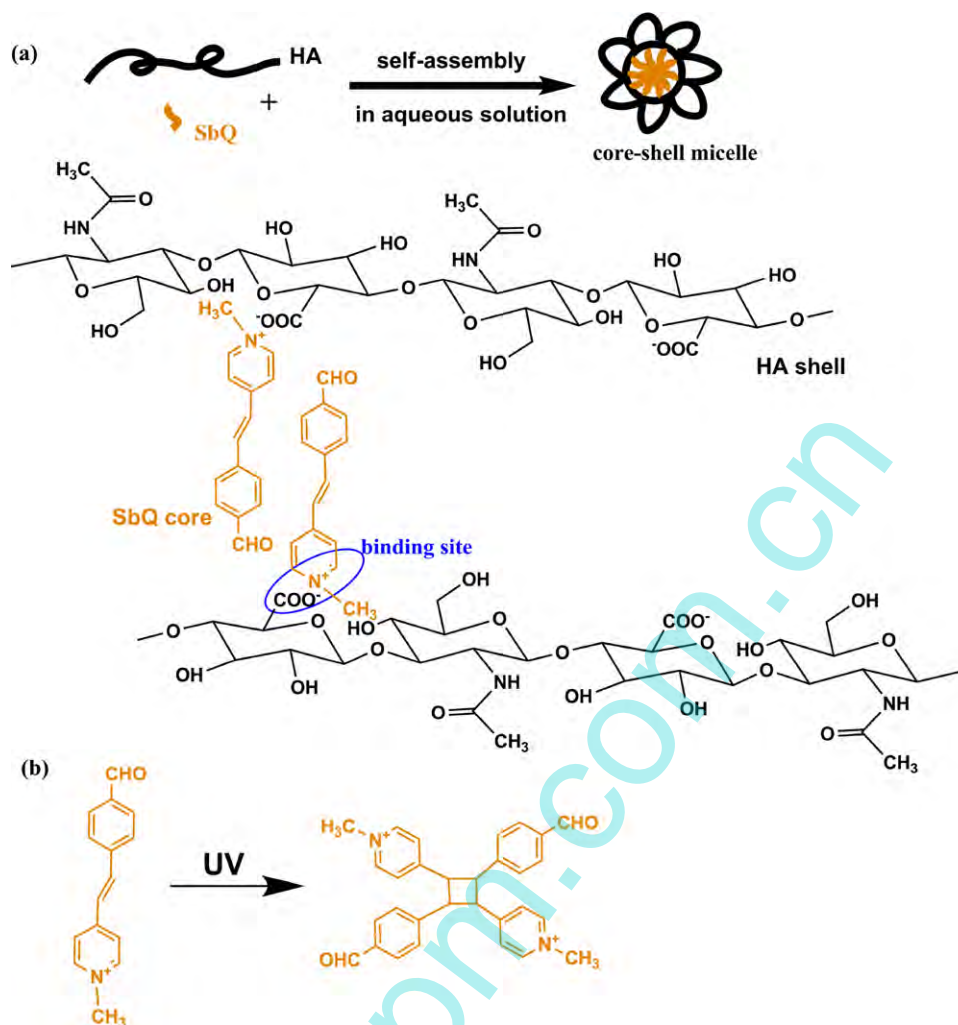


Fig. 1. Schematic illustration of micelle formation via self-assembly (a) and photo-dimerization mechanism of SbQ (b).

et al., 2009; Uhlich, Tomaschewski, & Komber, 1995). In addition, the physico-chemical behavior of SbQ in aqueous solution has also been investigated (Crowther & Eagland, 1997). However, no studies have to our knowledge been published on SbQ complexation with oppositely charged polyelectrolytes in aqueous solution.

In this paper, the self-assembly behavior between HA and SbQ in aqueous solution was investigated. A novel core-shell type micelle was obtained during the self-assembly process (Fig. 1a). This work also provides a new approach to the functionalization and modification of HA under mild conditions.

2. Experimental

2.1. Materials

1-Methyl-4-[2-(4-formylphenyl)-ethenyl]-pyridinium-methosulphate (SbQ) was provided by SHOWA KAKO Co. Ltd. (Japan). Sodium hyaluronate, with a viscosity average molecular weight of 22 kDa, was purchased from Zhenjiang Dongyuan Biology Technology Co. Ltd. (China). The chemicals were used as received without further purification. Deionized water was used for the preparation of all solutions.

2.2. Preparations

A HA solution was prepared by dissolving sodium hyaluronate in water, and stirring overnight at room temperature to ensure complete dispersion. Stock solutions of SbQ with different concentrations were prepared by dissolving SbQ in water. The HA solutions were mixed with a series of SbQ solutions in equal volume, ensuring the concentration of hyaluronate constant. All the mixtures were stored in glass bottles wrapped in aluminum foil package prior to use. The compositions of the mixtures (Z value) are expressed as the molar ratio of the positively charged SbQ and negatively charged carboxylate groups of HA, $Z = [\text{SbQ}]/[\text{COO}^-]$; they are reported for each experiment described here.

2.3. Measurements

Dynamic light scattering (DLS) measurements were carried out using an ALV-5000 laser light scattering spectrometer. All the solution samples were filtered through 0.45 μm Millipore filters to remove dust before the light scattering measurements. DLS measurements were performed at a fixed scattering angle of 90° at 25°C . The apparent hydrodynamic radius R_h was obtained using the CONTIN program.

ζ -Potentials of the micelle solutions were measured by a Malvern Zetasizer 2000 instrument. The solution samples were

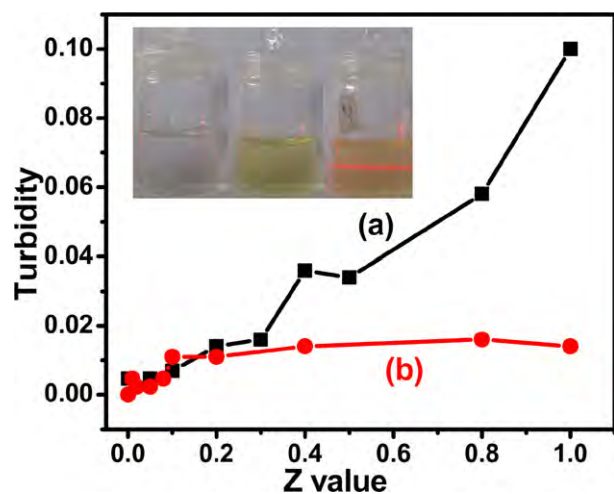


Fig. 2. (a) Turbidity of the mixtures of SbQ with the HA as a function of the Z value (the molar ratio between SbQ and carboxylate groups of HA). The mixtures were obtained by mixing HA solution ([HA] = 20 mg/ml) with SbQ solutions (from 0 to 16.7 mg/ml) in equal volume. The final concentration of HA in each mixture was 10 mg/ml. (b) For comparison, blank for pure SbQ without HA is given. The solution samples were obtained by mixing water (instead of HA solution) with SbQ solutions (in the same way as in (a)) in equal volume. The inset shows the tyndall light scattering experiment for three solution samples under the same experimental condition: HA solution (left), SbQ solution (middle) and HA/SbQ complex solution (Z = 1) (right).

injected into the instrument and the ζ -potential measurement was carried out at room temperature.

Transmission electron microscopy (TEM) was performed on a JEOL JEM-2100 microscope, operating at an acceleration voltage of 200 kV. The samples were prepared by drop-coating the micelle solution on the carbon-coated copper grid and drying at room temperature before observation.

For the atomic force microscopy (AFM) observations, 100 μ l of HA/SbQ micelle solution was placed on a clean mica surface and then air-dried overnight. The image was obtained with a Benyuan CSPM 4000 AFM system in the tapping mode with a scanned area of 5 μ m \times 5 μ m.

Turbidity was measured at different Z values during mixing of the HA with SbQ in aqueous solution. The absorbance of the mixture at 550 nm was measured by TU-1901 UV–vis spectrophotometry. The turbidity was calculated as turbidity = $1 - 10^{-A}$, where A is the UV absorbance of the mixture.

^1H NMR spectra were obtained at 25 $^\circ\text{C}$ with an AVANCE III 400 MHz Digital NMR spectrometer. Using D_2O as solvent.

To obtain cross-linked particles, the micelle solutions were irradiated under a POWER ARC UV 100 Lamp. The cross-linking process was tracked by TU-1901 UV–vis spectrophotometry.

3. Results and discussion

3.1. Behavior between HA and SbQ in aqueous solution

The self-assembly behavior between HA and SbQ in aqueous solution was studied using turbidity method. As shown in Fig. 2, the turbidity of the HA and SbQ mixtures gradually increases with the increasing of Z value (shown in Fig. 2a), indicating spontaneous formation of the HA/SbQ complex aggregates. In this case, blank experiment of a pure SbQ solution was designed for comparing with HA/SbQ solutions (Fig. 2b). From curve (b), we can exclude the possibility that turbidity changes are due to the formation of SbQ micelles. We hypothesize that, at low Z value, the SbQ molecules interact with the HA chains via electrostatic attraction, whereas at high Z value, the ordered micellar aggregates were formed owing

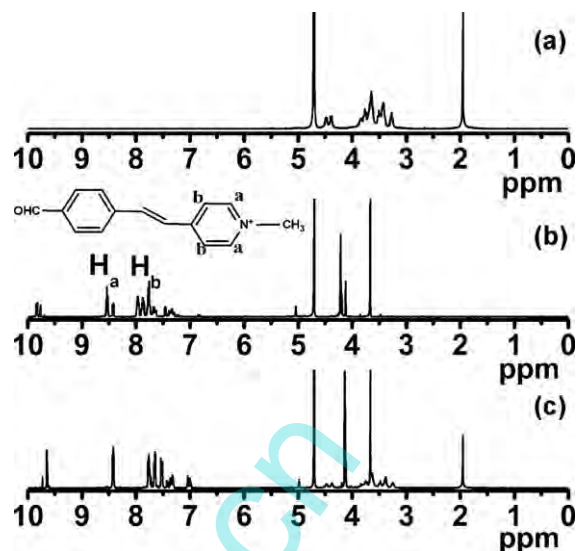


Fig. 3. ^1H NMR spectra of HA (a), SbQ (b) and HA/SbQ (c) measured in D_2O .

to hydrophobic interaction from the hydrophobic groups present in the SbQ structure.

The inset in Fig. 2 shows a simple Tyndall scattering experiment for an HA solution, a SbQ solution and an HA/SbQ complex solution (Z = 1), respectively. A strong light scattering signal was observed in the mixed solution of HA and SbQ, compared with pure HA and SbQ solutions, confirming that HA chains were aggregated by SbQ molecules to form the complex micelles.

The interaction between HA and SbQ was further confirmed from ^1H NMR spectra. As shown in Fig. 3, aromatic protons (H_a and H_b) on the pyridinium moiety of SbQ display upfield shift. This shift is due to the increase in electron density of the pyridinium moiety after binding with HA. Considering the above experimental evidence, electrostatic coordination of SbQ with HA forms the complex, where the binding site is carboxylate O and pyridinium N.

Fig. 4 depicts the dependence of the ζ -potential of HA/SbQ complex as a function of the Z value. It is seen that ζ -values are negative, which confirms that the shell moieties of the complex micelles contain $-\text{COO}^-$ groups. The change in the value of the ζ -potential is

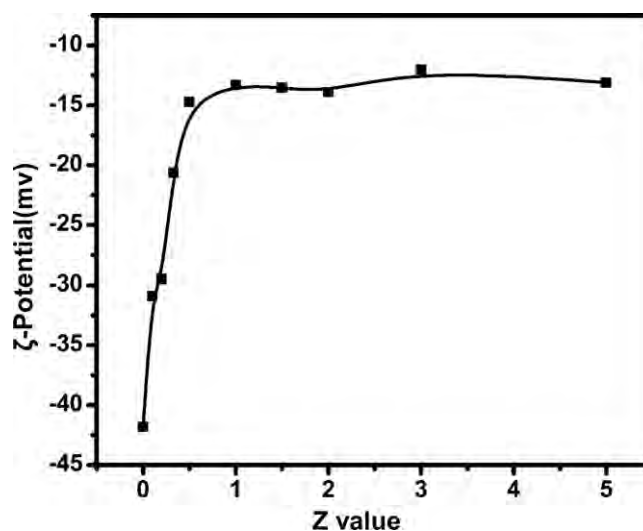


Fig. 4. ζ -Potential of HA/SbQ complex aggregates as a function of the molar ratio between SbQ and carboxylate groups of HA (Z value). [HA] = 0.5 mg/ml. The zeta measurement was performed at gradually increasing SbQ concentrations.

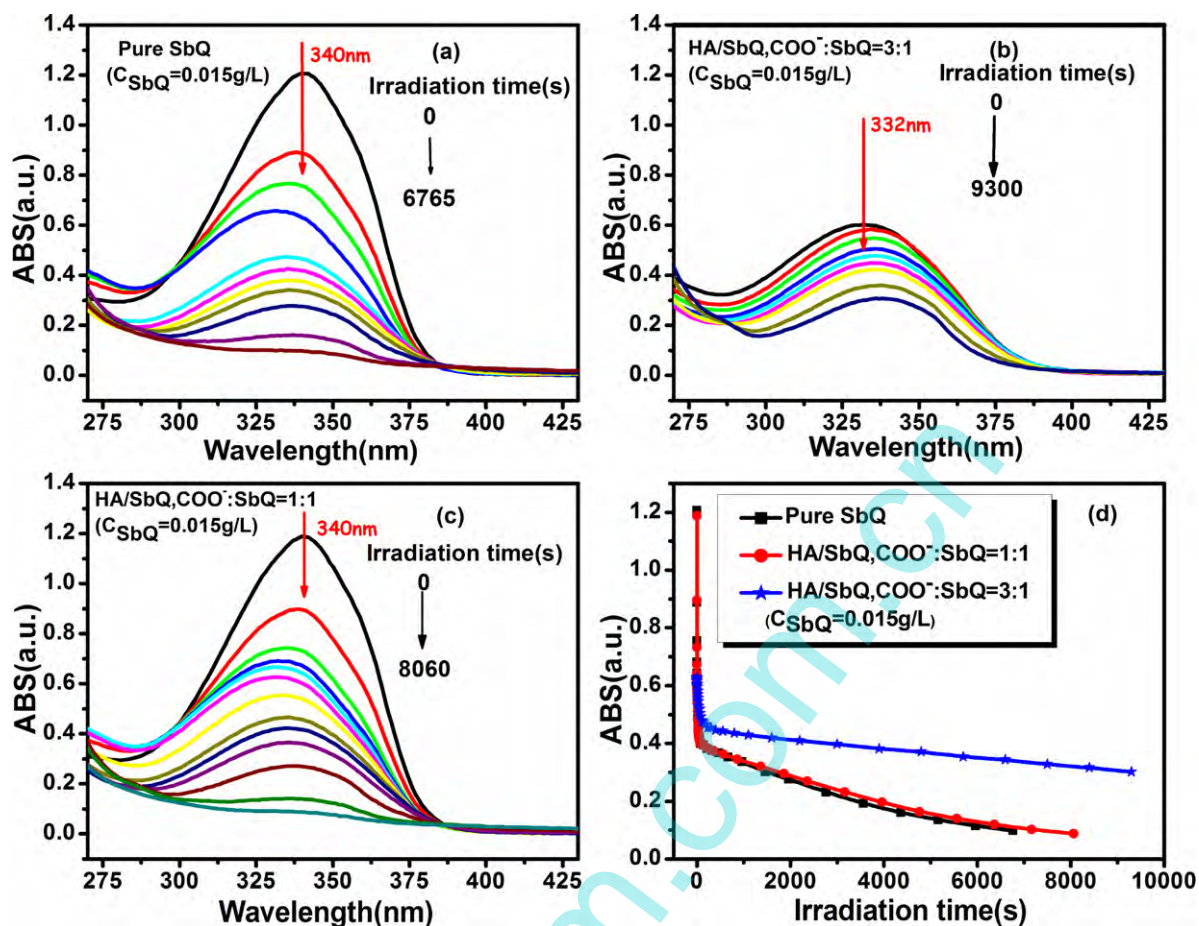


Fig. 5. UV-vis spectra of micellar aqueous solutions of three samples, showing the changes of UV absorption with different irradiation times under irradiation by POWER ARC UV 100 at a distance of 2 cm away: (a) pure SbQ $Z=0$, (b) HA/SbQ, $Z=1/3$, (c) HA/SbQ, $Z=1$ and (d) decrease of absorption at around 340 nm of all the samples under UV irradiation. The SbQ concentration for each sample was 0.015 g/l.

probably due to the binding of additional positively charged SbQ molecules to the HA chains. This change means that some negative charges from HA were neutralized with the addition of SbQ, while the rest of the carboxylate groups provided for the net negative charge of the micelles.

However, there appears to be a limit to the extent of SbQ binding by the HA chains, as the ζ -potential levels off at an almost constant value from $Z=0.5$. This limit is probably imposed by electrostatic repulsion of the headgroups of SbQ in the hydrophobic cores of the micelle particles (Solomatin et al., 2003). Therefore, only a part of negative charges are neutralized by SbQ molecules. Consequently, the excess SbQ molecules only exist in solution in the form of free molecules and small molecule micelles of pure SbQ instead of becoming incorporated into the micelle particles.

UV-vis spectroscopy was utilized to trace the photo-crosslinking process of pure SbQ solution and solutions containing SbQ bound HA micelles (Fig. 5). When the solution is exposed to UV light, the absorbance intensity at around 340 nm decrease continuously with increasing the irradiation time, indicating the dimerization of SbQ moieties. Furthermore, for sample (b), the maximum absorbance peak position blue-shifted to 332 nm, when the Z value reaches a ratio of three carboxylate groups to one SbQ. This shift is possibly due to that the conjugation of SbQ styryl structure is weakened with increasing HA concentration. In order to visualize the differences in behavior among the three samples, the changes of the characteristic absorption as a function of the irradiation time of these samples are depicted in the same figure (Fig. 5d). In contrast to sample (a) and (c), in sample (b), the HA/SbQ complex solution

obtained for $Z=1/3$, has the lowest photo-crosslinking reaction rate. This low crosslinking rate is observed because HA exists in the conformation of a random coil, with some SbQ molecules attached to the HA chains even at low Z value, and it is likely that SbQ molecules are far from each other, which inhibits the collision between SbQ molecules (Fig. 6a). However, at high Z value, spherical micelles with the inner core of SbQ are formed via electrostatic

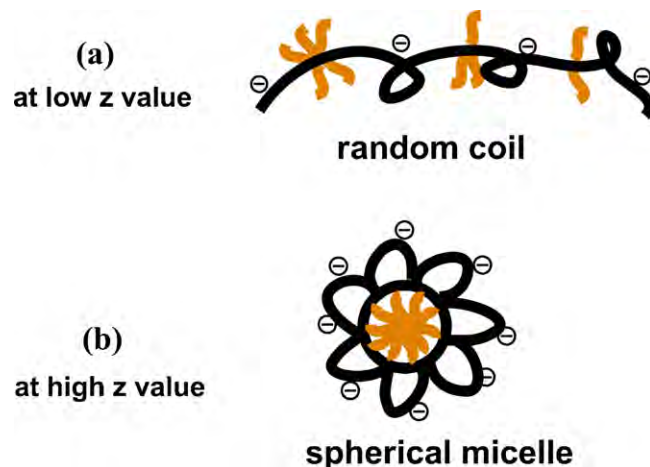


Fig. 6. Schematic illustration for the conformation of HA binding with SbQ: (a) coil at low Z value; (b) spherical micelle at high Z value.

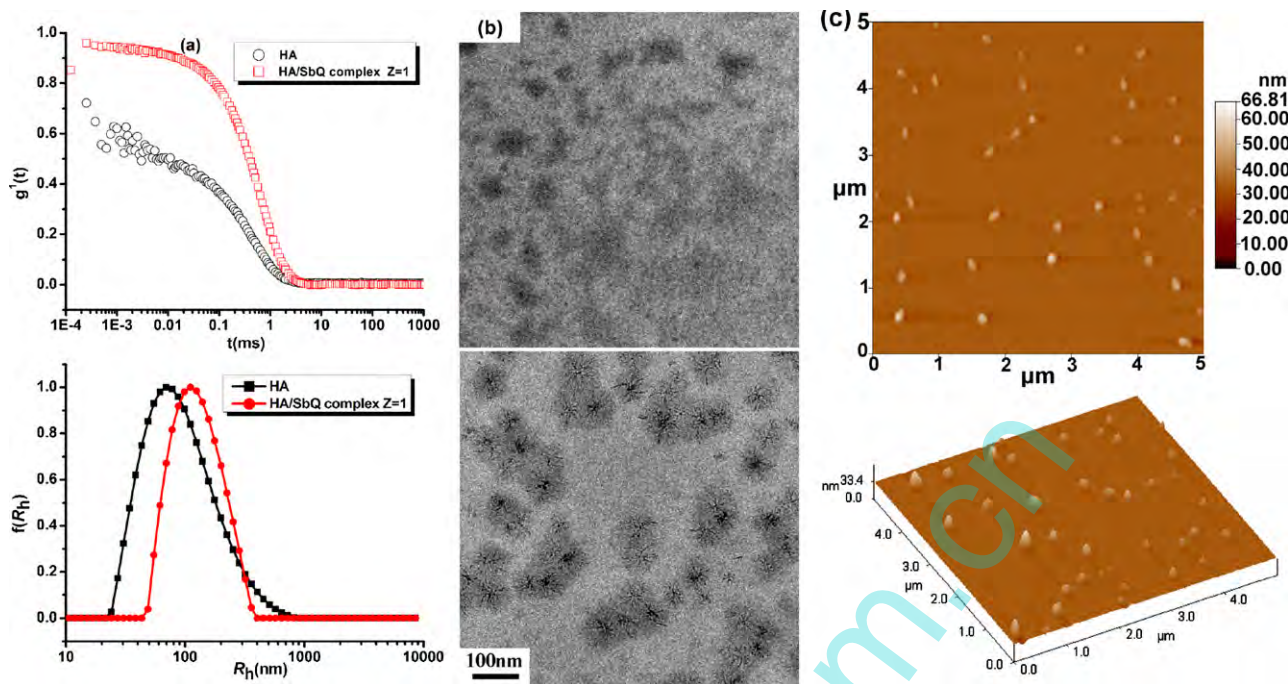


Fig. 7. (a) Correlation function for HA and HA/SbQ of $C_{HA} = 0.5$ mg/ml (up) and the corresponding distribution of hydrodynamic radius (down). (b) TEM images of HA (up) and HA/SbQ ($Z = 1$) (down) nanoparticles, respectively. (c) AFM topological 2D image (up) and 3D image (down) of HA/SbQ ($Z = 1$) nanoparticles.

self-assembly (Fig. 6b), and many SbQ molecules are located in the “sphere” within a short distance from each other. Consequently, chances of a collision between SbQ molecules are improved and a high dimerization rate is observed (Fig. 5c). This is also consistent with the above results.

3.2. Morphology and size of the HA/SbQ complex micelle ($Z = 1$)

Fig. 7a shows the $g^1(t)$ correlation function for the HA solution and HA/SbQ ($Z = 1$) micelle solution and the corresponding hydrodynamic radius R_h distribution $f(R_h)$. It is seen that the HA/SbQ complex aggregate has a higher R_h value than the pure HA aggregate. However, Ren et al. reported that the R_h values for the alginate/surfactant aggregates were always lower than that without surfactant (Ren et al., 2006). We hypothesize that, the benzene ring and pyridine ring in SbQ molecules would take a volume larger than the alkyl chains present in the usual surfactants. To visualize the HA/SbQ complex micelles, TEM and AFM images were obtained. TEM image of HA aggregates was also obtained for the comparison (Fig. 7b). The TEM image shows tight core-shell type micellar aggregates with an average diameter of around 75 nm. The AFM image also provides evidence for spherical morphology (Fig. 7c). The spherical morphology of the micelles probably results from the presence of hydrophobic interactions among the SbQ molecules, and the presence of excess negative charges on the chain. The hydrophobic species form the micellar core, while the negative charges provide the stabilization commonly encountered in small molecule SbQ micelles. The remaining free SbQ molecules form the counter ions in the solutions.

3.3. Photo-crosslinking of the HA/SbQ complex micelle ($Z = 1$)

As discussed above (Section 3.1, Fig. 5), the HA/SbQ complex micelle can be photo-crosslinked because of the photo-dimerization of SbQ. To investigate the photo-crosslinking process more intensively, the size of complex micelle at $Z = 1$ in aqueous

solution after irradiation was monitored by using an ALV-5000/E dynamic light scattering instrument. As shown in Fig. 8a, the size of micelle decreased gradually during UV irradiation, and the R_h value decreased from 124 nm (the initial value) to 70 nm after being exposed to UV light for 45 min. As commonly reported, photo-crosslinking induced shrinkage of micelle particles, leading to the decrease of R_h value (Jiang, Qi, Lepage, & Zhao, 2007; Liu et al., 2010). In our system, HA undergoes degradation which can also result in the decrease of R_h value. As a control experiment, the R_h value of pure HA was measured after different irradiation time and the size of pure HA decrease from 90 nm to 71 nm (Fig. 8b), a much smaller change compared to that of HA/SbQ micelles. Therefore, the decrease of the size of HA/SbQ micelles should be mainly attributed to the crosslinking of micelles.

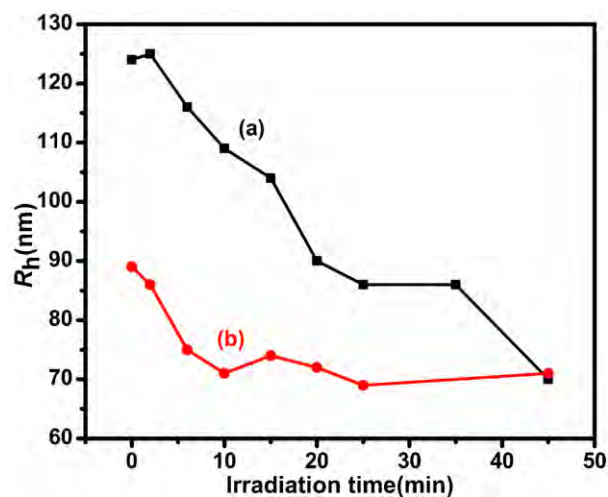


Fig. 8. R_h values of HA (a) and HA/SbQ (b) aggregates ($Z = 1$) upon irradiation at 365 nm detected by using an ALV-5000/E dynamic light scattering instrument at a HA concentration of 0.5 mg/ml.

4. Conclusions

In this study, a novel photo-crosslinkable micelle based on negatively charged hyaluronan (HA) and positively charged styrylpyridinium (SbQ) was obtained via an electrostatic self-assembly technique. The self-assembly behavior in aqueous solution was investigated. The strong association between HA and SbQ is driven by electrostatic attraction as well as the hydrophobic interactions between SbQ molecules. During the self-assembly process, core-shell type nano-sized micellar aggregates were observed, as characterized by TEM, AFM and DLS. UV spectra and DLS analysis confirmed that the micelles were photo-crosslinkable and that the photo-crosslinking of the inner core led to a decrease in size of the micelle particles. The preparation method of HA/SbQ complex micelles is simple, convenient and potentially applicable in cosmetics, photoactive materials, membrane, and biomaterials.

Acknowledgements

We thank Prof. Adi Eisenberg for correction and helpful suggestions. This work was supported by the National Science Foundation of China (grant no. 20974041) and State Key Laboratory of Food Science and Technology, Jiangnan University (SKLF-MB-200805).

References

- Annaka, M., Morishita, K., & Okabe, S. (2007). Electrostatic self-assembly of neutral and polyelectrolyte block copolymers and oppositely charged surfactant. *Journal of Physical Chemistry B*, *111*, 11700–11707.
- Antonietti, M. (1994). Polyelectrolyte-surfactant complexes: A new type of solid, mesomorphous material. *Macromolecules*, *27*, 6007–6011.
- Chang, K. S., Chang, C. K., Chou, S. F., Han, H. C., & Chen, C. Y. (2007). Characterization of a planar L-glutamate amperometric biosensor immobilized with a photo-crosslinkable polymer membrane. *Sensors and Actuators B*, *122*, 195–203.
- Chytil, M., & Pekar, M. (2009). Effect of new hydrophobic modification of hyaluronan on its solution properties: Evaluation of self-aggregation. *Carbohydrate Polymers*, *76*, 443–448.
- Claesson, P. M., Bergström, M., Dedinaite, A., Kjellin, M., Legrand, J. F., & Grillo, I. (2000). Mixtures of cationic polyelectrolyte and anionic surfactant studied with small-angle neutron scattering. *Journal of Physical Chemistry B*, *104*, 11689–11694.
- Cockburn, E. S., Stephen-Davidson, R., & Pratt, J. E. (1996). The photocrosslinking of styrylpyridinium salts via a [2 + 2]-cycloaddition reaction. *Journal of Photochemistry and Photobiology A: Chemistry*, *94*, 83–88.
- Cowman, M. K., & Matsuoka, S. (2005). Experimental approaches to hyaluronan structure. *Carbohydrate Research*, *340*, 791–809.
- Crowther, N. J., & Eagland, D. (1997). A styrylpyridinium salt in aqueous solution: Unusual solution behaviour. *Chemical Communications*, *1*, 103–104.
- Gao, H. J., Du, G. C., & Chen, J. (2006). Analysis of metabolic fluxes for hyaluronan acid (HA) production by streptococcus zooepidemicus. *World Journal of Microbiology and Biotechnology*, *22*, 399–408.
- Hansson, P., & Almgren, M. (1994). Interaction of alkyltrimethylammonium surfactants with polyacrylate and poly(styrenesulfonate) in aqueous solution: Phase behavior and surfactant aggregation numbers. *Langmuir*, *10*, 2115–2124.
- Hu, Z. J., Jonas, A. M., Varshney, S. K., & Gohy, J. F. (2005). Dilution-induced spheres-to-vesicles morphological transition in micelles from block copolymer/surfactant complexes. *Journal of the American Chemical Society*, *127*, 6526–6527.
- Jiang, J. Q., Qi, B., Lepage, M., & Zhao, Y. (2007). Polymer micelles stabilization on demand through reversible photo-cross-linking. *Macromolecules*, *40*, 790–792.
- Karlberg, M., Piculell, L., & Huang, L. (2007). Solubility of amylose/ionic surfactant complexes in dilute aqueous solutions: Dependence on surfactant concentration. *Carbohydrate Polymers*, *70*, 350–354.
- Kolarić, B., Jaeger, W., Hedicke, G., & Klitzing, R. V. (2003). Tuning of foam film thickness by different (poly)electrolyte/surfactant combinations. *Journal of Physical Chemistry B*, *107*, 8152–8157.
- Kujawa, P., Moraille, P., Sanchez, J., Badia, A., & Winnik, F. M. (2005). Effect of molecular weight on the exponential growth and morphology of hyaluronan/chitosan multilayers: A surface plasmon resonance spectroscopy and atomic force microscopy investigation. *Journal of the American Chemical Society*, *127*, 9224–9234.
- Kuntz, D. M., & Walker, L. M. (2007). Solution behavior of rod-like polyelectrolyte-surfactant aggregates polymerized from wormlike micelles. *Journal of Physical Chemistry B*, *111*, 6417–6424.
- Lee, H., Ahn, C. H., & Park, T. G. (2009). Poly[lactic-co-(glycolic acid)]-grafted hyaluronic acid copolymer micelle nanoparticles for target-specific delivery of doxorubicin. *Macromolecular Bioscience*, *9*, 336–342.
- Lee, H., Lee, K., & Park, T. G. (2008). Hyaluronic acid-paclitaxel conjugate micelles: Synthesis, characterization, and antitumor activity. *Bioconjugate Chemistry*, *19*, 1319–1325.
- Leonard, M., & Strey, H. H. (2010). Measurement of phase transition free energies in polyelectrolyte-surfactant complexes. *Macromolecules*, *43*, 4379–4383.
- Liu, X. Y., Yi, C. L., Zhu, Y., Yang, Y. Q., Jiang, J. Q., Cui, Z. G., et al. (2010). Pickering emulsions stabilized by self-assembled colloidal particles of copolymers of P(St-*alt*-MA*n*)-*co*-P(VM-*alt*-MA*n*). *Journal of Colloid and Interface Science*, *351*, 315–322.
- Liu, Y., Bolger, B., Cahill, P. A., & McGuinness, G. B. (2009). Water resistance of photocrosslinked polyvinyl alcohol based fibers. *Materials Letters*, *63*, 419–421.
- Mezei, A., Mészáros, R., Varga, I., & Gilányi, T. (2007). Effect of mixing on the formation of complexes of hyperbranched cationic polyelectrolytes and anionic surfactants. *Langmuir*, *23*, 4237–4247.
- Nam, S., Jeon, H., Kim, S. H., Jang, J., Yang, C., & Park, C. E. (2009). An inkjet-printed passivation layer based on a photocrosslinkable polymer for long-term stable pentacene field-effect transistors. *Organic Electronics*, *10*, 67–72.
- Ogrodowski, C. S., Hokka, C. O., & Santana, M. H. (2005). Production of hyaluronan acid by streptococcus. *Applied Biochemistry and Biotechnology*, *121–124*, 753–761.
- Onesippe, C., & Lagerge, S. (2008). Study of the complex formation between sodium dodecyl sulfate and hydrophobically modified chitosan. *Carbohydrate Polymers*, *74*, 648–658.
- Pitarresi, G., Pierro, P., Palumbo, F. S., Tripodo, G., & Giammona, G. (2006). Photo-cross-linked hydrogels with polysaccharide-poly(amino acid) structure: New biomaterials for pharmaceutical applications. *Biomacromolecules*, *7*, 1302–1310.
- Ren, B. Y., Gao, Y. M., Lu, L., Liu, X. X., & Tong, Z. (2006). Aggregates of alginates binding with surfactants of single ant twin alkyl chains in aqueous solutions: Fluorescence and dynamic light scattering studies. *Carbohydrate Polymers*, *66*, 266–273.
- Rinaudo, M. (2008). Main properties and current applications of some polysaccharides as biomaterials. *Polymer International*, *57*, 397–430.
- Solomatina, S. V., Bronich, T. K., Bargar, T. W., Eisenberg, A., Kabanov, V. A., & Kabanov, A. V. (2003). Environmentally responsive nanoparticles from block ionomer complexes: Effects of pH and ionic strength. *Langmuir*, *19*, 8069–8076.
- Szarpak, A., Cui, D., Dubreuil, F., De Geest, B. G., De Cock, L. J., Picart, C., et al. (2010). Designing hyaluronan acid-based layer-by-layer capsules as a carrier for intracellular drug delivery. *Biomacromolecules*, *11*, 713–720.
- Thalberg, K., & Lindman, B. (1989). Interaction between hyaluronan and cationic surfactants. *The Journal of Physical Chemistry*, *93*, 1478–1483.
- Uhlich, T., Tomaschewski, G., & Komber, H. (1995). Synthesis of a hydrophobised and photocrosslinkable prepolymer based on poly(vinyl alcohol). *Reactive and Functional Polymers*, *28*, 55–60.
- Vázquez, C. P., Boudou, T., Dulong, V., Nicolas, C., Picart, C., & Glinel, K. (2009). Variation of polyelectrolyte film stiffness by photo-cross-linking: A new way to control cell adhesion. *Langmuir*, *25*, 3556–3563.
- Yang, J. S., Chen, S. B., & Fang, Y. (2009). Viscosity study of interactions between sodium alginate and CTAB in dilute solutions at different pH values. *Carbohydrate Polymers*, *75*, 333–337.